

# E<sub>4</sub> Butterfly Complexes (E = P, As) as Chelating Ligands

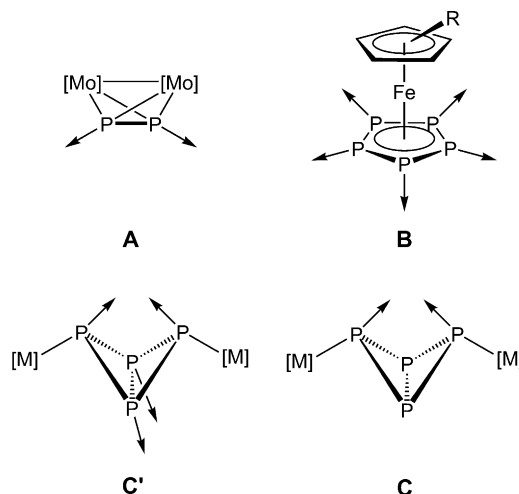
Christoph Schwarzmaier, Sebastian Heint, Gábor Balázs, and Manfred Scheer\*

Dedicated to Professor Maurizio Peruzzini on the occasion of his 60th birthday

**Abstract:** The coordination properties of new types of bidentate phosphane and arsane ligands with a narrow bite angle are reported. The reactions of  $[\{\text{Cp}^{\text{R}}\text{Fe}(\text{CO})_2\}_2(\mu, \eta^{1:1}\text{-P}_4)]$  (**1a**) with the copper salt  $[\text{Cu}(\text{CH}_3\text{CN})_4][\text{BF}_4]$  leads, depending on the stoichiometry, to the formation of the spiro compound  $[\{\{\text{Cp}^{\text{R}}\text{Fe}(\text{CO})_2\}_2(\mu_3, \eta^{1:1:1:1}\text{-P}_4)\}_2\text{Cu}^+][\text{BF}_4]^-$  (**2**) or the monoadduct  $[\{\{\text{Cp}^{\text{R}}\text{Fe}(\text{CO})_2\}_2(\mu_3, \eta^{1:1:2}\text{-P}_4)\}\{\text{Cu}(\text{MeCN})\}]^+[\text{BF}_4]^-$  (**3**). Similarly, the arsane ligand  $[\{\{\text{Cp}^{\text{R}}\text{Fe}(\text{CO})_2\}_2(\mu, \eta^{1:1}\text{-As}_4)]$  (**1b**) reacts with  $[\text{Cu}(\text{CH}_3\text{CN})_4][\text{BF}_4]$  to give  $[\{\{\text{Cp}^{\text{R}}\text{Fe}(\text{CO})_2\}_2(\mu_3, \eta^{1:1:1:1}\text{-As}_4)\}_2\text{Cu}^+][\text{BF}_4]^-$  (**5**). Protonation of **1a** occurs at the “wing tip” phosphorus atoms, which is in line with the results of DFT calculations. The compounds are characterized by spectroscopic methods (heteronuclear NMR spectroscopy and IR spectrometry) and by single-crystal X-ray diffraction studies.

**P<sub>n</sub>** ligand complexes are an interesting class of compounds with growing potential for application in different fields.<sup>[1]</sup> Based on the coordinatively active lone pairs on the P atoms, the coordination properties attract considerable interest and were studied extensively for the majority of existing complexes. One of the first investigations were carried out by Sacconi et al., who used  $[(\text{triphos})\text{Co}(\eta^3\text{-P}_3)]$  (triphos =  $\text{CH}_3\text{C}(\text{CH}_2\text{PPh}_2)_3$ ) as a ligand.<sup>[2]</sup> In our group, the use of the complexes  $[\text{Cp}_2\text{Mo}_2(\text{CO})_4(\mu, \eta^{2:2}\text{-P}_2)]^{[3]}$  (type **A**) and  $[\text{Cp}^{\text{R}}\text{Fe}(\eta^5\text{-P}_5)]$  (type **B**;  $\text{Cp}^{\text{R}} = \text{C}_5\text{Me}_5$ ,  $\text{C}_5(\text{CH}_2\text{C}_6\text{H}_5)_5$ ,  $\text{C}_5(4\text{-}n\text{BuC}_6\text{H}_4)_5$ ) as building blocks in supramolecular chemistry has been extensively investigated.<sup>[4]</sup> However, regarding white phosphorus activation,<sup>[1,5]</sup> one of the first steps of activation is the cleavage of a P–P bond under formation of a butterfly-like moiety, which can be fixed by one or two covalent bound fragments.<sup>[6]</sup>

Since the isolation of the first transition-metal-stabilized bridging P<sub>4</sub> butterfly complex  $[\{\text{Cp}^{\text{R}}\text{Fe}(\text{CO})_2\}_2(\mu, \eta^{1:1}\text{-P}_4)]$  (type **C**),<sup>[7]</sup> the reactivity under thermolytic<sup>[8]</sup> and photolytic<sup>[7,9]</sup> conditions as well as its reactivity towards various alkynes<sup>[10]</sup> has been intensively investigated. In contrast, their coordination behavior towards Lewis acids has not been studied to date. Formally, all four P atoms could further coordinate (type **C'**) to Lewis acids, or just the two wing-tip phosphorus atoms in complexes of type **C** could bear accessible lone pairs to act itself as bidentate ligand with a narrow bite angle revealing



large steric bulk. On the other hand, only the bridgehead P atoms could perform further coordination.

To confirm the accessibility of the lone pairs in type **C'** compounds, the frontier molecular orbitals of the model complex  $[\{\text{CpFe}(\text{CO})_2\}_2(\mu, \eta^{1:1}\text{-P}_4)]$  were calculated using DFT methods at the BP86/def-SVP level of theory (Figure 1). The HOMO (highest occupied molecular orbital) as well as the HOMO–1 are mainly localized at the P<sub>4</sub> framework as well as at the iron atoms. The HOMO contains contributions from the lone pairs at the “wing-tip” P atoms and shows a bonding

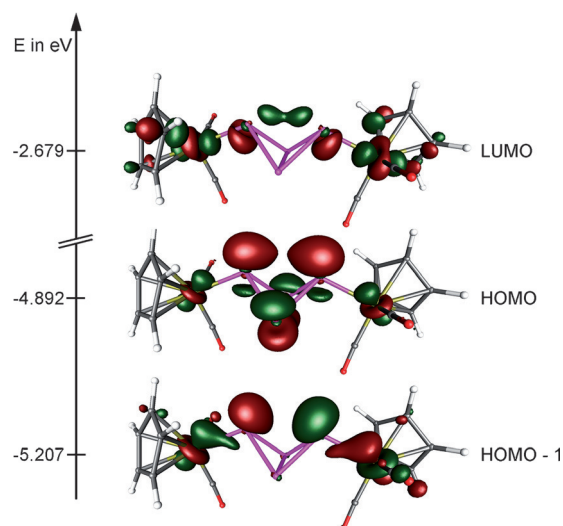


**Figure 1.** Illustration of the HOMO, HOMO–1, and LUMO of the model complex  $[\{\text{CpFe}(\text{CO})_2\}_2(\mu, \eta^{1:1}\text{-P}_4)]$  calculated at the BP86/def-SVP level of theory.

[\*] Dr. C. Schwarzmaier, Dr. S. Heint, Dr. G. Balázs, Prof. Dr. M. Scheer  
Institut für Anorganische Chemie der Universität Regensburg  
93040 Regensburg (Germany)  
E-mail: Manfred.Scheer@ur.de

Supporting information for this article is available on the WWW under <http://dx.doi.org/10.1002/anie.201506784>.

overlap between the two “bridgehead” P atoms. The HOMO–1 can be seen as a combination of the lone pairs at the wing-tip P atoms and an Fe d-orbital with a slight antibonding character with respect to the Fe–P bond. However, the position of the filled orbitals should allow an appreciable interaction between the wing-tip P atoms of the butterfly complex and a Lewis acid. Additionally, the LUMO (lowest unoccupied molecular orbital) can be found in between the two wing-tip phosphorus atoms, which could allow back-bonding from the Lewis acid to the butterfly complex.

These new results encouraged us to investigate the coordination behavior of compounds of type **C** towards unsaturated metal centers. These type **C** compounds of phosphorus and arsenic are now easily accessible in high quantities,<sup>[8b,9]</sup> which facilitated the proposed studies. The coordination chemistry studies were driven by the question of whether a further activation of the E<sub>4</sub> butterfly unit could occur, or if this unusual framework could serve as a novel chelating ligand. Herein, we report on detailed studies of the reactions of  $[\{\text{Cp}^{\text{III}}\text{Fe}(\text{CO})_2\}_2(\mu, \eta^{1:1}\text{-P}_4)]$  (**1a**,  $\text{Cp}^{\text{III}} = \eta^5\text{-C}_5\text{H}_2\text{tBu}_3$ ) with the monovalent copper salt  $[\text{Cu}(\text{CH}_3\text{CN})_4][\text{BF}_4]$  in various stoichiometries as well as the first investigations of the coordination behavior of the arsenic compound  $[\{\text{Cp}^{\text{III}}\text{Fe}(\text{CO})_2\}_2(\mu, \eta^{1:1}\text{-As}_4)]$  (**1b**). Moreover, the protonation of the P<sub>4</sub> butterfly was studied experimentally and by DFT calculations.

The reaction of two equivalents of **1a** with one equivalent of  $[\text{Cu}(\text{MeCN})_4]^+[\text{BF}_4]^-$  leads to the selective formation of the red spiro compound  $[\{\{\text{Cp}^{\text{III}}\text{Fe}(\text{CO})_2\}_2(\mu_3, \eta^{1:1:1:1}\text{-P}_4)\}_2\text{Cu}]^+[\text{BF}_4]^-$  (**2**) (yield of single crystals: 54%; Figure 2). In contrast, the reaction in a 1:1 stoichiometry affords the red-orange monoadduct  $[\{\text{Cp}^{\text{III}}\text{Fe}(\text{CO})_2\}_2(\mu_3, \eta^{1:1:2}\text{-P}_4)\{\text{Cu}(\text{MeCN})\}]^+[\text{BF}_4]^-$  (**3**).

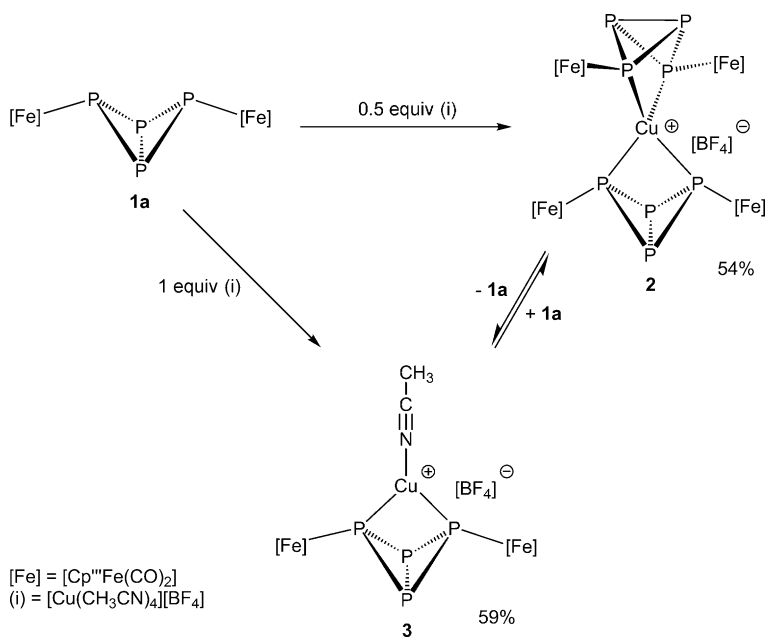


**Figure 2.** Reaction of the butterfly complex **1a** with  $[\text{Cu}(\text{MeCN})_4]^+[\text{BF}_4]^-$  with different stoichiometry.

In **3** only three acetonitrile ligands are substituted by one butterfly complex. Compounds **2** and **3** can be isolated as red and reddish orange solids, respectively. Both products show good solubility in  $\text{CH}_2\text{Cl}_2$  and THF but are insoluble in hexane. The crystal structure of **2** confirms the proposed chelating coordination of the copper(I) cation by two molecules of **1a** (Figure 3) by their wing-tip P atoms. The

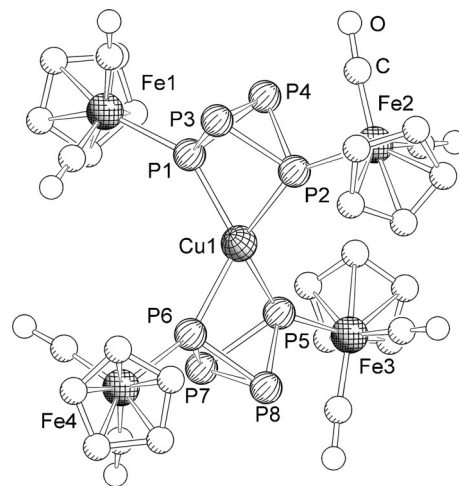


**Figure 3.** Cationic part of the structure of **2**·2THF in the crystal. Solvent molecules, H atoms, and tBu groups are omitted for clarity.<sup>[17]</sup>

central  $\text{Cu}^+$  atom is coordinated in a distorted tetrahedral manner. The molecular structure of **3** (Figure 4) shows the coordination of one molecule of **1a** also as a chelate towards one  $\text{Cu}^+$  cation. The coordination sphere of copper is completed by one acetonitrile ligand, resulting in a trigonal-planar arrangement (Figure 4). The Cu–P bond lengths in **2** vary from 2.3630(8) Å to 2.4268(8) Å. This is slightly longer than in the archetypal compound  $[(\text{dppe})_2\text{Cu}]^+[\text{ClO}_4]^-$  (2.259(2) Å–2.301(2) Å; dppe = bis(diphenylphosphino)ethane)<sup>[11]</sup> but compares well to the bond lengths in the dppm-containing compound  $[(\text{dppm})(\text{POP})\text{Cu}]^+[\text{BF}_4]^-$  (POP = bis[2-(diphenylphosphino)phenyl]ether; dppm = bis(diphenylphosphino)methane) with 2.333(3) Å and 2.425(4) Å.<sup>[12]</sup>

The Cu1–P1 and Cu1–P2 bond lengths in **3** of 2.3224(7) Å and 2.2891(6) Å are shorter than in **2**. Therefore, the copper cation is coordinated more tightly by the butterfly complex. This might be caused by the reduced steric bulk on one side of the central Cu atom in **3**, which allows a better interaction between the Lewis acid and **1a**. In **2** the Fe–P bond lengths are in the range from 2.3059(8) Å to 2.3380(8) Å and are shorter than in the starting material **1a** (2.348(2) Å and 2.355(2) Å).<sup>[8a]</sup> This might be raised by the contribution of the HOMO–1 for the coordination of the copper cation. As this MO possesses an antibonding character with respect to the Fe–P bond, the electron withdrawing effect of the Lewis acid strengthens the Fe–P bond and decreases the

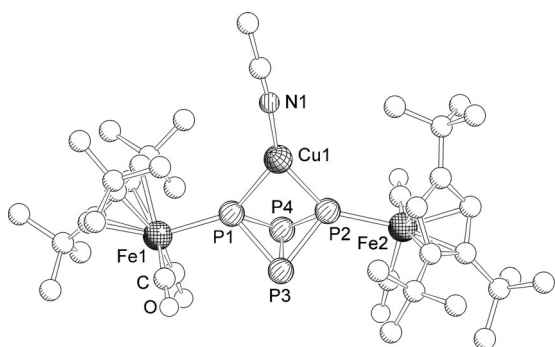


**Figure 4.** Cationic part of the structure of **3** in the crystal. Hydrogen atoms and the  $[\text{BF}_4]^-$  counterion are omitted for clarity.<sup>[17]</sup>

bond length. This effect is even more conspicuous in **3**, where the Fe–P bond lengths decrease to 2.2928(6) Å and 2.2845(6) Å. Here the reduced steric bulk of compound **3** could also play a role.

While in both cases the P–P bonds between the coordinating and non-coordinating P atoms are essentially the same as those in **1a**, the P3–P4 and P7–P8 bonds in **2** (2.176(1) Å and 2.175(1) Å) and **3** (P3–P4 2.1792(8) Å) are shorter than the corresponding bond in **1a** (2.209(2) Å). The distance of the wing-tip P atoms (**2**: 2.833(1) Å, 2.846(1) Å; **3**: 2.8135(8) Å) are also shorter compared to **1a** (2.964(3) Å). This means the butterfly frameworks are contracted by the interaction with the copper cation. However, the bite angles in **2** are small at 72.51(3)° and 72.71(3)°, and compare well to the dppm bite angle in  $[(\text{dppm})(\text{POP})\text{Cu}]^+[\text{BF}_4]^-$  (73.3(1)°). As the bite angle as well as the Cu–P bonds in  $[(\text{dppm})(\text{POP})\text{Cu}]^+[\text{BF}_4]^-$  and **2** are very similar, the butterfly complex **1a** may be regarded as sterically demanding, inorganic analogue of dppm.

The positive-ion ESI mass spectra of **2** and **3** do not show any copper-containing fragments, indicating rather weak Cu–P interactions. The IR spectra (KBr) of both compounds reveal blue-shifted carbonyl stretching bands compared to the starting material **1a** (**1a**:  $\tilde{\nu}$  = 2000, 1950  $\text{cm}^{-1}$ ;[8a] **2**:  $\tilde{\nu}$  = 2008, 1960, 1930  $\text{cm}^{-1}$ ; **3**:  $\tilde{\nu}$  = 2009, 2000, 1962, 1956  $\text{cm}^{-1}$ ). This points to slightly stronger C–O bonds and consequently weaker  $\pi$ -backbonding. This can be readily explained by an electron-withdrawing effect of the coordinated copper(I) cation. In the IR spectrum of **3**, one weak band at  $\tilde{\nu}$  = 2285  $\text{cm}^{-1}$  for the terminal acetonitrile ligand is observed.

The  $^1\text{H}$  NMR spectrum ( $\text{CD}_2\text{Cl}_2$ ) of **2** shows three sharp singlets at  $\delta$  = 1.42, 1.44, and 4.82 ppm for the freely rotating  $\text{Cp}'''$  ligands. In the  $^{31}\text{P}\{^1\text{H}\}$  NMR spectrum ( $\text{CD}_2\text{Cl}_2$ ) two triplets of an  $\text{A}_2\text{M}_2$  spin system at  $\delta$  = –81.2 and –282.0 ppm ( $^1J_{\text{PP}}$  = 181 Hz) appear that correspond to the wing-tip and the bridgehead phosphorus atoms of the butterfly complex, respectively. While the first is shifted upfield compared to the signal in **1a**, the latter is shifted downfield (**1a**:  $\delta$  = –75.2 and –322.3 ppm). Additionally, the signals show a broadening at their base, indicating a more complicated spin system. Hence, VT NMR investigations were performed to shed more light in the spin system of **2**. Upon cooling to 193 K, the chemical shift of both signals is nearly unchanged. While the triplet at  $\delta$  = –81.2 ppm is only slightly broadened, the

upfield-shifted signal at  $\delta$  = –282.0 ppm shows severe line broadening at 213 K ( $\omega_{1/2}$  = 443 Hz) and is only detected as a broad singlet ( $\omega_{1/2}$  = 795 Hz) at 193 K (Figure 5c). The broadening of the upfield shifted signal seems to be a result of a hindered rotation of the  $\text{Cp}'''$  ligands. However, the VT NMR spectra do not allow a further analysis of the spin system of **2**.

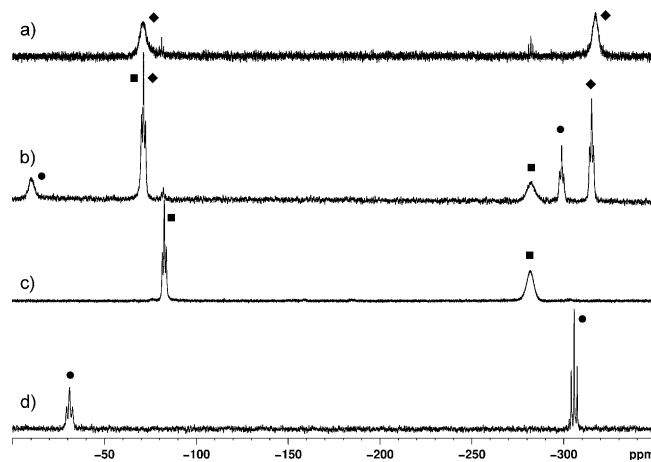


**Figure 5.**  $^{31}\text{P}\{^1\text{H}\}$  NMR spectra ( $\text{CD}_2\text{Cl}_2$ ) of a) **3** at 300 K, b) **3** at 193 K, c) **2** at 193 K, and d) **4** at 193 K; ■ = **2**, ◆ = **3**, ● = **4**.

In the  $^1\text{H}$  NMR spectrum ( $\text{CD}_2\text{Cl}_2$ ) of **3**, one typical set of signals for the  $\text{Cp}'''$  ligands are detected. Additionally, a sharp singlet for the acetonitrile ligand appears at  $\delta$  = 2.36 ppm. The  $^{31}\text{P}\{^1\text{H}\}$  NMR spectrum ( $\text{CD}_2\text{Cl}_2$ ) of a freshly prepared sample of **3** at room temperature reveals two broad signals at  $\delta$  = –71.0 ( $\omega_{1/2}$  = 608 Hz) and –317.2 ppm ( $\omega_{1/2}$  = 625 Hz), indicating dynamic behavior in solution (Figure 5a). Furthermore, two rather small sharp triplets for complex **2** are observed. The molar ratio of the mono- and bis-chelate complexes can be determined to about 24:1. After six hours, the molar ratio is lowered to about 14:1 and does not change further upon time. Hence, a dynamic ligand exchange must have taken place in solution (Figure 2).

To further investigate the equilibrium of **3** in solution a  $^{31}\text{P}\{^1\text{H}\}$  NMR spectrum at 193 K was recorded, revealing a total of five signals at  $\delta$  = –11.4 ppm (br s,  $\omega_{1/2}$  = 609 Hz), –72.4 ppm (t,  $^1J_{\text{PP}}$  = 176 Hz), –283.3 ppm (br s,  $\omega_{1/2}$  = 800 Hz), –300.0 ppm (t,  $^1J_{\text{PP}}$  = 177 Hz), and –316.3 ppm (t,  $^1J_{\text{PP}}$  = 177 Hz; Figure 5b). The integral intensity ratio of the signals is 1:3:1:1:2, indicating three species in solution. The signal at  $\delta$  = –72.4 results from superimposition of two signals with integral intensities of 2:1. The signals at  $\delta$  = –72.4 and –283.3 ppm can be assigned to complex **2**. Furthermore, the chemical shifts of the triplets at  $\delta$  = –72.4 and –316.3 ppm compare well to the broad signals found in the room-temperature spectrum of **3**. They are therefore assigned to the monochelate complex **3**. The formation of **2** from two molecules of **3** formally affords the release of a  $[\text{Cu}(\text{MeCN})_2]^+$  fragment which acts as a Lewis acid in solution and can interact with both complexes **2** or **3**. The resulting product gives rise to the signals at  $\delta$  = –11.4 and –300.0 ppm. To

clarify the nature of these signals, the butterfly complex **1a** was reacted with two equivalents of  $[\text{Cu}(\text{MeCN})_4]^+[\text{BF}_4]^-$  and the  $^{31}\text{P}\{^1\text{H}\}$  NMR spectrum of the solution ( $\text{CD}_2\text{Cl}_2$ ) was recorded at 193 K (Figure 5d). It shows two triplets at  $\delta = -31.0$  and  $-305.6$  ppm with a coupling constant of  $^1J_{\text{PP}} = 194$  Hz, which are reminiscent of the two unassigned signals in the  $^{31}\text{P}\{^1\text{H}\}$  NMR spectrum of **3** at 193 K. The discrepancy in the chemical shift is most likely a result of the different temperatures of the measurements and the amount of acetonitrile in the solution. The NMR investigations of **3** indicate ligand exchange reactions in solution affording the bis-chelate complex **2** as well as the new compound **4**. Unfortunately, regardless of many attempts **4** could not be isolated and further characterized. Therefore the identity could not be confirmed unambiguously. For steric reasons, the coordination of the  $[\text{Cu}(\text{MeCN})_2]^+$  via the bridgehead P atoms of the butterfly framework seems reasonable (type C'). Alternatively, the down-field shift of about 60 ppm of the signal of the wing-tip P atoms compared to **2** and **3** might indicate the coordination of an additional  $\text{Cu}^+$  to these P atoms.

In the late 1950s, Ahrlund et al. reported on a generally weaker donor character of arsane ligands compared to their phosphane derivatives.<sup>[13]</sup> This trend is exemplified well by the increased dissociation tendency of arsane complexes of copper(I) compared to the corresponding phosphane complexes.<sup>[14]</sup> This can also be observed for chelating arsane and phosphane ligands.<sup>[15]</sup> Hence, the coordination behavior of the  $\text{As}_4$  butterfly complexes  $[\{\text{Cp}''\text{Fe}(\text{CO})_2\}_2(\mu, \eta^{1:1}-\text{As}_4)]$  (**1b**) towards copper(I) cations moved into the focus of our interest.

The reaction of two equivalents of **1b** with  $[\text{Cu}(\text{MeCN})_4]^+[\text{BF}_4]^-$  leads to the formation of  $[\{\{\text{Cp}''\text{Fe}(\text{CO})_2\}_2(\mu_3, \eta^{1:1:1:1}-\text{As}_4)\}_2\text{Cu}]^+[\text{BF}_4]^-$  (**5**) in moderate yields. This is in agreement with the analogous reaction with contribution of **1a** forming **2**. Complex **5** is obtained as dark red solid that has good solubility in  $\text{CH}_2\text{Cl}_2$  or THF but is insoluble in hexane. Note, by using different stoichiometries only **5** could be obtained.

The IR spectrum of **5** (KBr) reveals two sharp absorption bands at  $\tilde{\nu} = 1991$  and  $1953\text{ cm}^{-1}$  of which only the latter one is blue-shifted by  $10\text{ cm}^{-1}$  compared to **1b**. This is in contrast to the blue-shift of both absorption bands in the  $\text{P}_4$  derivative **2** and points to a weaker interaction between **1b** and the copper(I) cation. In the  $^1\text{H}$  NMR spectrum ( $\text{CD}_2\text{Cl}_2$ ) shows an appropriate set of signals for **5**, without any abnormalities.

Crystals of **5** are obtained as solvate with two molecules THF by slow diffusion of hexane into THF solutions. The  $\text{As1-Cu1-As2}$  and  $\text{As5-Cu1-As6}$  angles ( $76.74(2)^\circ$  and  $76.36(1)^\circ$ ) are larger than the  $\text{P-Cu-P}$  angles in **2** ( $72.51(3)^\circ$  and  $72.71(3)^\circ$ ), which is due to the larger  $\text{As}_4$  butterfly ligand (Figure 6). The  $\text{Cu-As}$  bonds range from  $2.4559(4)\text{ \AA}$  to  $2.4988(5)\text{ \AA}$  and are about  $0.1\text{ \AA}$  longer than the  $\text{Cu-As}$  bonds in the chelate complex  $[(\text{pdma})_2\text{Cu}]^+$  ( $\text{pdma} = \text{C}_6\text{H}_4(\text{AsMe}_2)_2$ ) ( $2.360(1)\text{ \AA}$ ).<sup>[16]</sup> A reason for this might be the large steric bulk of **1b** compared to the rather small  $\text{pdma}$  ligand. Complex **5** shows the same tendencies in the  $\text{As-As}$  bond lengths compared to **1b** as complex **2** in comparison to **1a**. The most obvious change is also the shorter distance

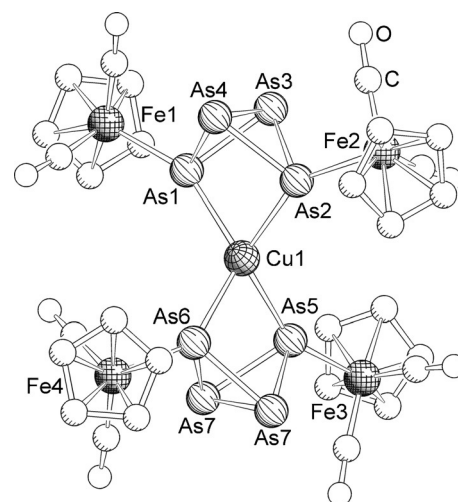


**Figure 6.** Cationic part of the structure of **5**·2 THF in the crystal. H atoms, *t*Bu groups, and the  $[\text{BF}_4]^-$  counterion are omitted for clarity.<sup>[17]</sup>

between the wing-tip As atoms caused by the coordination of the Lewis acid  $\text{Cu}^+$ . Furthermore, the  $\text{Fe-As}$  bond lengths are shorter ( $2.4033(4)\text{ \AA}$ – $2.4294(4)\text{ \AA}$ ) than in **1b** ( $2.443(3)\text{ \AA}$ – $2.458(3)\text{ \AA}$ ). This is in good agreement with the shortening of the  $\text{Fe-P}$  bond in the  $\text{P}_4$  chelate complexes **2** and **3** and this indicates a contribution of the HOMO–1 orbital (see Figure 1) for the coordination of the copper(I) cation also in the arsenic case.

To gain more insight to the reaction behavior of butterfly complexes, we also investigated the reaction of **1a** with  $[(\text{Et}_2\text{O})_n\text{H}]^+[\text{A}]^-$  ( $[\text{A}]^- = [\text{BF}_4]^-$ ,  $n = 1$ ;  $[\text{A}]^- = [\text{Al}(\text{OC}(\text{CF}_3)_3)_4]^-$ ,  $n = 2$ ). Upon addition of either  $[(\text{Et}_2\text{O})\text{H}]^+[\text{BF}_4]^-$  in  $\text{Et}_2\text{O}$  or  $[(\text{Et}_2\text{O})_2\text{H}]^+[\text{Al}(\text{OC}(\text{CF}_3)_3)_4]^-$  in  $\text{CH}_2\text{Cl}_2$  to **1a** in hexane, an orange precipitate or solution forms, respectively. The orange substances were identified as  $[\{\text{Cp}''\text{Fe}(\text{CO})_2\}_2(\mu, \eta^{1:1}-\text{P}_4)\text{H}]^+[\text{A}]^-$  ( $6^+\text{A}^-$ ).  $^{31}\text{P}\{^1\text{H}\}$  NMR spectra in  $\text{CD}_2\text{Cl}_2$  of  $6^+\text{A}^-$  show identical signals, regardless of the counterion  $[\text{A}]^-$ . The spectra show a triplet at  $\delta = -311.8$  ppm ( $^1J_{\text{PP}} = 230$  Hz) and a broad triplet at  $\delta = 6.6$  ppm ( $^1J_{\text{PP}} = 230$  Hz). At lower temperatures the broadened signal splits into a broad pseudo-quartet ( $J = 214$  Hz) in the  $^{31}\text{P}$  NMR spectrum, indicating a proton bound to the wing-tip P atoms. Additionally, the triplet at  $\delta = -311.8$  ppm splits into a triplet of doublets ( $^2J_{\text{HP}} = 4$  Hz).  $^{31}\text{P}\{^1\text{H}\}$  NMR investigations at various temperatures first show a further broadening upon cooling (Figure 7). At 233 K the signal at  $\delta = 6.6$  ppm splits into two signals. Finally reaching 193 K the two signals sharpen, resulting in two sets of doublets of triplets at  $\delta = 16.8$  ppm and  $-5.5$  ppm, respectively. An additional coupling of the signal at  $\delta = -5.5$  ppm is observed in the  $^{31}\text{P}$  NMR spectrum, confirming one proton attached to one of the wing-tip P atoms.

The  $^1\text{H}$  VT NMR spectra of  $6^+$  only show one set of signals for the  $\text{Cp}''$  ligands but no signal for the proton bound to a P atom (see the Supporting Information). However, upon cooling, the signal of the two protons attached to the  $\text{Cp}''$  ring splits into two singlets confirming the non-equivalence of the  $\{\text{Cp}''\text{Fe}(\text{CO})_2\}$  fragments. This behavior could not be observed for the *t*Bu groups. This is probably due to the low



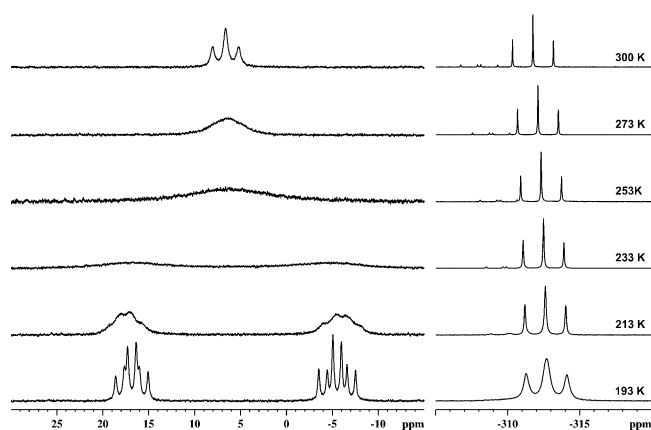


**Figure 7.**  $^{31}\text{P}\{^1\text{H}\}$  NMR ( $\text{CD}_2\text{Cl}_2$ ) of  $6^+\text{A}^-$  at various temperatures (top) and  $^{31}\text{P}$  NMR ( $\text{CD}_2\text{Cl}_2$ ) at 193 K (bottom). Only regions of interest are depicted. Complete spectra at 300 K and 193 K as well as  $^{31}\text{P}$  NMR spectra are depicted in the Supporting Information.

perturbation in the magnetic field of the *t*Bu groups induced by the hydrogen atom.

By diffusion of hexane into a THF solution of  $6^+[\text{Al}(\text{OC}(\text{CF}_3)_3)_4]^-$ , orange crystals form. Though the quality is insufficient for a good-quality structure refinement, the crystal could be measured and a structure solution could be obtained. A variety of anions  $[\text{A}]^-$  and crystallization conditions were tried without success to improve the crystal quality. The cell parameters and a model picture of  $6^+[\text{Al}(\text{OC}(\text{CF}_3)_3)_4]^-$  can be found in the Supporting Information. Interestingly, also here the unsymmetrical  $\text{H}^+$  coordination to the wing-tip P atoms was found, which is in agreement with the DFT calculations. These calculations for  $6^+$  clearly show that  $\text{H}^+$  is attached to one of the wing-tip phosphorus atoms (Figure 8). The geometry in which  $\text{H}^+$  is symmetrically bound to both wing-tip phosphorus atoms represents a transition state. This lies in the model compound  $[(\text{CpFe}(\text{CO})_2)_2(\mu_2\eta^{1,1}-\text{P}_4)\text{H}]^+$  higher in energy with  $54.99 \text{ kJ mol}^{-1}$ . The isomer of  $6^+$  in which  $\text{H}^+$  binds to the bridgehead phosphorus atoms (Supporting Information, Figure S5) is energetically less favored by  $66.08 \text{ kJ mol}^{-1}$ . Accordingly the attachment of  $\text{H}^+$  to the bridgehead phosphorus atoms can be ruled out.

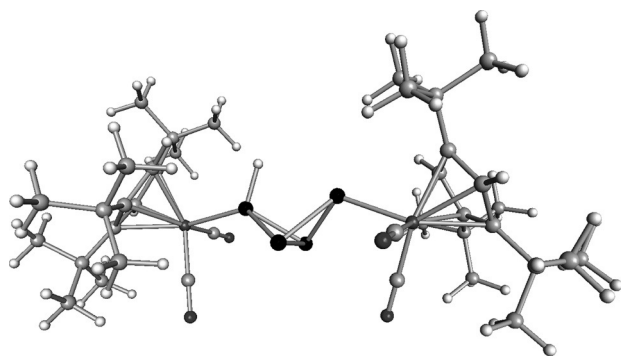


**Figure 8.** Optimized geometry of  $6^+$  at the B3LYP/def2-TZVP (for P) and def2-SVP (for all other atoms) level of theory.

In conclusion, we have shown the potential of the  $\text{E}_4$  ( $\text{E} = \text{P}, \text{As}$ ) butterfly complexes **1a** and **1b** to act as chelating ligands with small bite angles for copper(I) cations. In both cases, a homoleptic bis-chelate complex (**2** and **5**) could be obtained showing distorted tetrahedral coordination for copper. For **1a** also the mono chelating compound **3** could be isolated. Complex **3** shows dynamic behavior in solution under ligand exchange. Furthermore, it was possible to selectively protonate **1a** at one wing-tip P atom of the butterfly core. These results indicate that butterfly complexes can generally be used as ligands for transition metals and other Lewis acids. The large steric bulk of the butterfly complexes together with their small bite angle could make them interesting ligands for catalytic applications.

## Acknowledgements

This work was supported by the Deutsche Forschungsgemeinschaft (DFG). S.H. and C.S. are grateful for a Ph.D. fellowship of the Fonds der Chemischen Industrie.

**Keywords:** arsenic · butterfly complexes · chelate ligands · phosphorus · protonation

**How to cite:** *Angew. Chem. Int. Ed.* **2015**, *54*, 13116–13121  
*Angew. Chem.* **2015**, *127*, 13309–13314

- [1] a) B. M. Cossairt, N. A. Piro, C. C. Cummins, *Chem. Rev.* **2010**, *110*, 4164–4177; b) M. Caporali, L. Gonsalvi, A. Rossini, M. Peruzzini, *Chem. Rev.* **2010**, *110*, 4178–4235; c) M. Scheer, G. Balázs, A. Seitz, *Chem. Rev.* **2010**, *110*, 4236–4256; d) N. A. Giffin, J. D. Masuda, *Coord. Chem. Rev.* **2011**, *255*, 1342–1359; e) S. Khan, S. S. Sen, H. W. Roesky, *Chem. Commun.* **2012**, *48*, 2169–2179.
- [2] M. Di Vaira, L. Sacconi, *Angew. Chem. Int. Ed. Engl.* **1982**, *21*, 330–342; *Angew. Chem.* **1982**, *94*, 338–351.
- [3] a) M. Scheer, L. J. Gregoriades, M. Zabel, J. Bai, I. Krossing, G. Brunklaus, H. Eckert, *Chem. Eur. J.* **2008**, *14*, 282–295; b) M. Scheer, L. Gregoriades, J. Bai, M. Sierka, G. Brunklaus, H. Eckert, *Chem. Eur. J.* **2005**, *11*, 2163–2169; c) S. Welsch, L. J. Gregoriades, M. Sierka, M. Zabel, A. V. Virovets, M. Scheer, *Angew. Chem. Int. Ed.* **2007**, *46*, 9323–9326; *Angew. Chem.* **2007**, *119*, 9483–9487; d) B. Attenberger, S. Welsch, M. Zabel, E. Peresypkina, M. Scheer, *Angew. Chem. Int. Ed.* **2011**, *50*, 11516–11519; *Angew. Chem.* **2011**, *123*, 11718–11722.
- [4] a) J. Bai, A. V. Virovets, M. Scheer, *Science* **2003**, *300*, 781–783; b) M. Scheer, J. Bai, B. P. Johnson, R. Merkle, A. V. Virovets, C. E. Anson, *Eur. J. Inorg. Chem.* **2005**, 4023–4026; c) M. Scheer, A. Schindler, R. Merkle, B. P. Johnson, M. Linseis, R. Winter, C. E. Anson, A. V. Virovets, *J. Am. Chem. Soc.* **2007**, *129*, 13386–13387; d) M. Scheer, A. Schindler, C. Groeger, A. V. Virovets, E. V. Peresypkina, *Angew. Chem. Int. Ed.* **2009**, *48*, 5046–5049; *Angew. Chem.* **2009**, *121*, 5148–5151; e) A. Schindler, C. Heindl, G. Balázs, C. Gröger, A. V. Virovets, E. V. Peresypkina, M. Scheer, *Chem. Eur. J.* **2012**, *18*, 829–835; f) F. Dielmann, A. Schindler, S. Scheuermayer, J. Bai, R. Merkle, M. Zabel, A. V. Virovets, E. V. Peresypkina, G. Brunklaus, H. Eckert, M. Scheer, *Chem. Eur. J.* **2012**, *18*, 1168–1179; g) F. Dielmann, C. Heindl, F. Hastreiter, E. V. Peresypkina, A. V. Virovets, R. M. Gschwind, M. Scheer, *Angew. Chem. Int. Ed.* **2014**, *53*, 13605–13608; *Angew. Chem.* **2014**, *126*, 13823–13827; h) F. Dielmann, M. Fleischmann, C. Heindl, E. V. Peresypkina, A. V. Virovets, R. M. Gschwind, M. Scheer, *Chem. Eur. J.* **2015**,

- 21, 6208–6214; i) C. Heindl, S. Heinl, D. Lüdeker, G. Brunklaus, W. Kremer, M. Scheer, *Inorg. Chim. Acta* **2014**, 422, 218–223; j) C. Schwarzmaier, A. Schindler, C. Heindl, S. Scheuermayer, E. V. Peresypkina, A. V. Virovets, M. Neumeier, R. Gschwind, M. Scheer, *Angew. Chem. Int. Ed.* **2013**, 52, 10896–10899; *Angew. Chem.* **2013**, 125, 11097–11100.
- [5] M. Serrano-Ruiz, A. Romerosa, P. Lorenzo-Luis, *Eur. J. Inorg. Chem.* **2014**, 1587–1598.
- [6] a) J. E. Borger, A. W. Ehlers, M. Lutz, J. C. Slootweg, K. Lammertsma, *Angew. Chem. Int. Ed.* **2014**, 53, 12836–12839; *Angew. Chem.* **2014**, 126, 13050–13053; b) D. Holschumacher, T. Bannenberg, K. Ibrom, C. G. Daniliuc, P. G. Jones, M. Tamm, *Dalton Trans.* **2010**, 39, 10590–10592.
- [7] O. J. Scherer, G. Schwarz, G. Wolmershäuser, *Z. Anorg. Allg. Chem.* **1996**, 622, 951–957.
- [8] a) O. J. Scherer, T. Hilt, G. Wolmershäuser, *Organometallics* **1998**, 17, 4110–4112; b) S. Heinl, M. Scheer, *Chem. Sci.* **2014**, 5, 3221–3225.
- [9] a) T. Hilt, Ph.D. thesis, university of Kaiserslautern (Kaiserslautern), **1999**; b) C. Schwarzmaier, A. Y. Timoshkin, G. Balázs, M. Scheer, *Angew. Chem. Int. Ed.* **2014**, 53, 9077–9081; *Angew. Chem.* **2014**, 126, 9223–9227.
- [10] a) M. Scheer, S. Deng, O. J. Scherer, M. Sierka, *Angew. Chem. Int. Ed.* **2005**, 44, 3755–3758; *Angew. Chem.* **2005**, 117, 3821–3825; b) O. J. Scherer, T. Hilt, G. Wolmershäuser, *Angew. Chem. Int. Ed.* **2000**, 39, 1425–1427; *Angew. Chem.* **2000**, 112, 1483–1485.
- [11] P. Comba, C. Katsichtis, B. Nuber, H. Pritzkow, *Eur. J. Inorg. Chem.* **1999**, 777–783.
- [12] O. Moudam, A. Kaeser, B. Delavaux-Nicot, C. Duhayon, M. Holler, G. Accorsi, N. Armaroli, I. Seguy, J. Navarro, P. Destruel, J.-F. Nierengarten, *Chem. Commun.* **2007**, 3077–3079.
- [13] S. Ahrland, J. Chatt, N. R. Davies, *Q. Rev. Chem. Soc.* **1958**, 12, 265–276.
- [14] S. J. Lippard, J. J. Mayerle, *Inorg. Chem.* **1972**, 11, 753–759.
- [15] G. Salem, A. Schier, S. B. Wild, *Inorg. Chem.* **1988**, 27, 3029–3032.
- [16] O. M. Abu Salah, M. I. Bruce, P. J. Lohmeyer, C. L. Raston, B. W. Skelton, A. H. White, *J. Chem. Soc. Dalton Trans.* **1981**, 962–967.
- [17] CCDC 1411084 (**2**), 1411085 (**3**), and 1411086 (**5**) contain the supplementary crystallographic data for this paper. These data are provided free of charge by The Cambridge Crystallographic Data Centre.

Received: July 22, 2015

Published online: September 2, 2015